ELECTROLUMINESCENCE

DISPLAYS, ELECTROLUMINESCENT

PHOSPHORS, ELECTROLUMINESCENT

In the broad sense of the word, electroluminescence refers to all phenomena where light is generated under the influence of an electric field in a material. Light-emitting diodes and organic semiconductors, which emit light when electrons and holes recombine with each other, correspond to this definition but are discussed elsewhere in this encyclopedia. The scope of this article is limited to solid state electroluminescent devices which use a high electric field to generate light. We distinguish two different classes: powder electroluminescent devices and thin-film electroluminescent devices. Since the former are only useful for not very demanding low-end applications, mainly as flexible light sources, most of this article is devoted to the thin-film type, with special attention to the electrical characteristics.

POWDER ELECTROLUMINESCENT DEVICES

Electroluminescence (EL) was first observed by Destriau in 1936, when he applied a high field to a ZnS powder material that had been treated with Cu. Based on this discovery, two kinds of powder electroluminescent devices were developed: the ac and the dc type (1–3).

In the ac type, a thick layer of dielectric binding material in which grains of ZnS:Cu are dispersed is located between two electrodes (4), as shown in Fig. 1(a). As a result of high temperature treatment, the ZnS grains contain needlelike copper sulfide precipitates which are rather conductive. When a voltage is applied between the electrodes, charge carriers move along these precipitates and make the field distribution very inhomogeneous. Near the ends of the needlelike precipitates the field in the ZnS material is very high, and electrons or holes are injected into the normally insulating ZnS. These charges then recombine with holes or electrons that have been captured in the ZnS layer during the previous voltage pulse, and the energy is released as a photon. The color of the light emission is modified by using additional dopant materials like Cl, Al, or Mn. The brightness versus voltage characteristic, shown in Fig. 1(d) is not very steep, but the conversion efficiency of electrical power to light is relatively high (3 lumen/W). The main applications for ac powder electroluminescence are flat and flexible light sources, even wires. An important drawback of these devices is the trade-off between lifetime and luminance level: due to the diffusion of copper in ZnS the precipitates degenerate in the high field, and the efficiency of the device is reduced. Nevertheless by using micro-encapsulated phosphors and limiting the luminance the technology is still useful in many low-end applications.

The dc type powder electroluminescent device is based on ZnS grains coated with copper sulfide (5). The structure consists of a thick layer of this conducting powder material between two electrodes. During a forming process, a thin copperfree highly resistive ZnS layer is created near the anode, as in Fig. 1(b). When a voltage is applied over the structure the field in this thin ZnS layer can be of the order of 10^8 *V/m*, and electrons can be accelerated and excite dopant atoms, as for example Mn. When the excited atom returns to the ground state, a photon is emitted. It is possible to arrange the dc powder devices in a matrix display with row electrodes on one side and column electrodes on the other side of the powder layer. Due to the steep brightness versus voltage characteristic of Fig. 1(d), a display with high contrast can be obtained. The devices are then driven with short voltage pulses instead of a true dc voltage. Compared to the other electroluminescent technologies, the efficiency is relatively low (0.5 lumen/W).

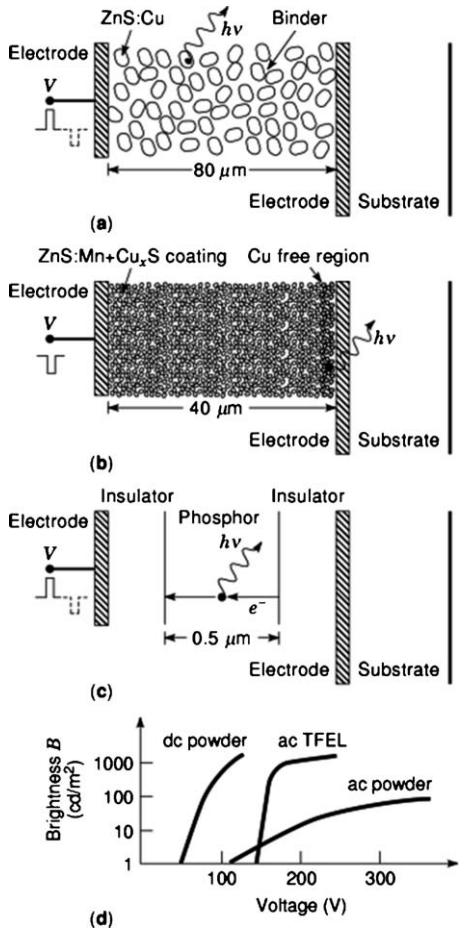

Figure 1. (a) In an ac powder EL device, charge transport and light generation are inside the ZnS:Cu grains. (b) In a dc powder EL device, light is generated in the Cu free region near the anode, where electrons are accelerated. (c) In the ac TFEL device, electrons move back and forth through the entire phosphor layer and excite dopant atoms. (d) The typical brightness versus voltage is given at 500 Hz for the ac devices, and at 500 Hz, 1% duty cycle for the dc powder device. The dc powder EL and the ac TFEL devices have a steep characteristic and can be used in matrix displays.

THIN-FILM ELECTROLUMINESCENT DEVICES

Thin-film electroluminescent devices (TFELD) consist of a stack of five layers on a substrate: conductor/insulator/phosphor/insulator/conductor/substrate (2–7) as in Fig. 1(c). The phosphor layer consists of a polycrystalline material like ZnS or SrS, which is doped with atoms such as Mn, Tb, or Ce; a common notation for the resulting phosphor is for example ZnS:Mn. The dopant atoms have a concentration of the order of 1 mol%, and play a critical role in the light generation process. The insulator layers are usually made of amorphous oxides and behave like capacitors. It is essential that they can withstand large electrical fields without damage. The conductor layers are patterned and the regions where they overlap define the active light-emitting areas of the device.

To obtain light emission from a thin-film electroluminescent device, a voltage pulse must be applied over the two conductors. As long as the amplitude V_e of the voltage pulse is below the threshold voltage V_t, which is in the order of 100 V, the phosphor layer can be considered as an insulator. The device then behaves like a simple capacitor. When the electric field in the phosphor layer is above the threshold value, electrons at the insulator/phosphor interface at the side of the negative potential are liberated and move toward the other side of the phosphor layer, as shown in Fig. 1(c). In the high electric field, the electrons gain energy and can use this energy to excite the dopant atoms in the phosphor. When an excited dopant atom relaxes from the excited state to the ground state, it can emit a photon. The spectrum of the emitted light is mainly determined by the energy levels of the dopant atom. The electrons can not move through the insulator material and are trapped at the phosphor/insulator interface, at the side of the positive potential. The trapped electrons create a polarization electric field in the phosphor layer which inhibits the transfer of more electrons. The next voltage pulse that is applied over the electrodes has the opposite polarity, so that the flow of electrons in the phosphor layer is reversed. For an applied ac voltage the electrons move back and forth in the phosphor layer, each time dopant atoms are excited, and light is generated.

The main application for TFELDs is in flat panel displays (1, 2). The row electrodes on one side of the structure and the column electrodes on the other side form a matrix of rectangular pixels. One of the conductors is transparent, so that the light can be emitted perpendicular to the substrate surface. Typically there are hundreds of rows and columns in the matrix, and arbitrary images can be displayed by applying a sequence of voltage pulses to the line and column electrodes. This is possible because the brightness versus voltage characteristic in Fig. 1(d) is very nonlinear. A rate of 60 light pulses per second is fast enough to give the impression of a continuous light flow. The displays are usually monochrome, based on the bright yellow-orange ZnS:Mn phosphor, or have a limited number of colors. TFEL displays have a wide viewing angle, high contrast, long life, and can operate in a wide temperature range. Often they are used to display textual or graphical information in combination with electronic equipment.

ELECTRICAL BEHAVIOR OF THIN-FILM ELECTROLUMINESCENT DEVICES

General Equations

In a TFELD the lateral dimensions are larger than the thickness and the electrical fields and currents are directed along the x-axis, perpendicular to the substrate. Charge and current are proportional with the area of the device $A[m^2]$, and in the following description charge, current, and capacitance are given per unit area. Figure 2 illustrates the definitions of the following electrical parameters: the externally applied voltage $V_e[V]$, the external current density $J_e[A/m^2]$, the abscissa $x[m]$, the phosphor layer thickness $d_p[m]$, $\varepsilon_p[F/m]$ the permittivity of the phosphor, the capacitances C_p, C_{i1} and C_{i2} $[F/m^2]$ of the phosphor and insulator layers, the electric field $E(x)[V/m]$, the current density $J(x)[A/m^2]$, the space charge density $\rho(x)[C/m^3]$, and the surface charges Q_a, Q_b, and Q_e, $[C/m^2]$. The total charge in the phosphor layer, including Q_a, Q_b and the space charge, is normally zero and the charges on the external electrodes have opposite signs: Q_e and $-Q_e$. The capacity of the two insulator layers together is C_i, and the total capacitance of the TFELD is $C_e = C_i\, C_p/(C_i + C_p)$. The order of magnitude for the above quantities are: $V_e \cong 100\,V, d_p \cong 5.10^{-7}\ m, \varepsilon_p \cong 8.10^{-11}\ F/m, C_e \cong 10^{-4}\ F/m^2, E \cong 10^8\ V/m, \rho \cong 10^4\ C/m^3, Q_e \cong 10^{-2}\ C/m^2$, the current densities can have different values, depending on the time derivative of the voltage. The gradient of the field $E(x)$ and the current density $J(x)$ are determined by the space charge (8–10: p. 28):)

$$\frac{dE}{dx} = \frac{\rho}{\varepsilon}; \frac{dJ}{dx} = -\frac{d\rho}{dt}$$

There are different processes which determine the current density $J(x)$ in the phosphor layer. The most important ones are shown in the energy band diagram of Fig. 2:

1. Tunneling of electrons from deep states at the phosphor/insulator interface, through a triangular potential barrier, to the conduction band of the phosphor layer (8–11). The probability for this process depends strongly on the width of the potential barrier, and thus on the value of the electric field. For interface states with depth ζ [eV] below the conduction band, the tunneling current J_t is proportional with:

$$J_t \sim \exp(-\frac{\alpha\zeta^{3/2}}{|E|})$$

   with α a constant.
2. Excitation of dopant atoms by electrons which have gained energy in the electric field. This is the process that will yield the light emission and is discussed in the following paragraph (7, 9). An energy of about 3 eV is required, and the resulting visible photon has an energy of about 2.5 eV.
3. Ionization of deep donor states by electrons (3, 11). The electrons that are created in this way move toward the interface at the anodic side, and contribute to the current density $J(x)$. Other processes, like the creation of electron-hole pairs by hot electrons, the

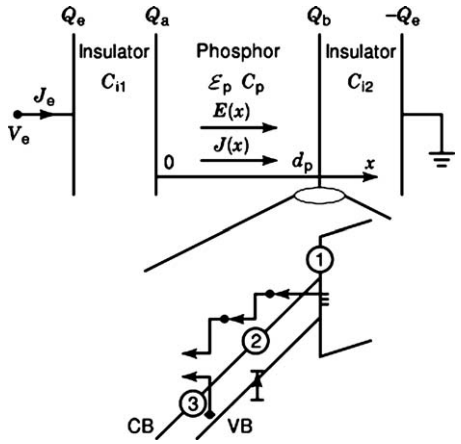

Figure 2. Cross section of a model for a thin-film electroluminescent device, showing the location of the surface charge densities Q_e, Q_a, and Q_b, the space charge density ρ, electric field E, and current density J. The lower part of the figure shows the energy band diagram for the enlarged region near the phosphor interface for $E > 0$ For ZnS, the conduction band (CB) is 3.6 eV above the valence band (VB). Electrons tunnel from the cathodic interface (1); they can impact-excite dopant atoms (2) or ionize donor states (3).

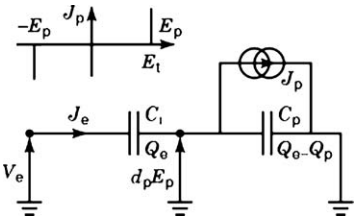

Figure 3. Equivalent circuit for a thin-film electroluminescent device with two capacitors and a current source J_p, representing the average current in the phosphor layer. The insulator capacitor C_i carries a charge Q_e, the phosphor capacitor C_p a charge $Q_e - Q_p$, and the voltage over the capacitor C_p is $d_p E_p$. The additional diagram with the abrupt relation between the current J_p and the field E_p corresponds to the ideal model.

trapping of electrons in deep states at the phosphor/insulator interface states, or the recombination with ionized donors, are also possible.

The TFELD corresponds with the equivalent circuit of Fig. 3, where C_i represents the insulator layers and C_p with a current source J_p in parallel represents the phosphor layer (12). In this circuit, E_p and J_p are respectively the average electric field and average current density in the phosphor layer (11, 12):

$$E_p = \frac{1}{d_p}\int_0^{d_p} E(x)dx : J_p = \frac{1}{d_p}\int_0^{d_p} J(x)dx$$

The charge density Q_p is the dipole moment of the charges in the phosphor layer, divided by the thickness:

$$Q_p = Q_b + \int_0^{d_p} \frac{x}{d_p}\rho(x)dx : \quad \text{with} \quad J_p = \frac{dQ_p}{dt}$$

At the external electrodes, the voltage V_e, the charge Q_e and the current density $J_e = dQ_e/dt$ can be measured. As can be seen from the equivalent circuit of Fig. 3, they are related with the average current and field in the phosphor layer (9, 12) by the equations:

$$V_e = \frac{Q_e}{C_i} + d_p E_p; \quad J_e = C_e\frac{dV_e}{dt} + \frac{C_i}{C_i + C_p}J_p$$

The latter equation shows that the current J_e has a capacitive contribution and a conductive contribution, due to the current J_p. In general, the current density J_p is not a simple function of the average field E_p, because the field can be inhomogeneous and different charge transfer processes occur. From the equivalent circuit in Fig. 3, the following equation can also be derived (11):

$$V_e = \frac{Q_p}{C_i} + (\frac{C_p}{C_i} + 1)d_p E_p$$

it shows that the average field E_p is due not only to the applied voltage V_e, but also the charge Q_p gives a contribution, sometimes called the depolarization field.

Ideal Model

The idealized electrical model assumes that there is no space charge in the phosphor layer, and that the tunneling current is an abrupt function of the electric field: zero below the threshold field E_t and arbitrarily large above E_t. According to Eq. (1), the current J and the field E are then homogeneous and equal to average values J_p and E_p. The idealized relation between the average current J_p and the average field E_p is given in Fig. 3 (1–3). It can be implemented in the equivalent circuitry by substituting the current source by two back-to-back Zener diodes with breakdown voltage $d_p\ E_t$. During breakdown the voltage over C_p is clamped to $d_p\ E_t$, and the current is limited by the insulator layers as can be seen from Eqs. (4) and (6):

$$J_p = J_e = C_i\frac{dV_e}{dt} \quad \text{for} \quad |E_p| = E_t$$

At a given time, either E_p or Q_p is constant and the variation of the other quantity can be derived from Eq. (6). When we apply a symmetric periodic voltage waveform with amplitude V_m, then no charge will be transferred as long as the voltage remains below the threshold voltage V_t, from Eq. (6):

$$V_t = (\frac{C_p}{C_i} + 1)d_p E_t$$

When the amplitude V_m is above the threshold voltage, then the extreme values for Q_p can be found from Eq. (6) with $V_e = \pm V_m$ and $E_p = \pm E_t$. In steady state (ss), during each half period a charge $\Delta Q_{p,ss}$ is transferred:

$$\Delta Q_{p,ss} = \begin{cases} 0 & V_m < V_t \\ 2C_i(V_m - V_t) & V_m > V_t \end{cases}$$

Curve 1 in Fig. 4(c) shows the transferred charge as a function of the amplitude of the voltage V_m. In practice, there is a soft transition region between both linear parts, as in curve 2 of Fig. 4(c), because tunneling is not really an abrupt process [see Eq. (2)].

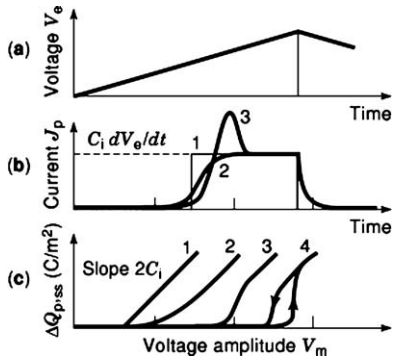

Figure 4. (a) Triangular voltage pulse $V_e(t)$ and (b) corresponding current pulses $J_p(t)$ with different shapes: (1) rectangular for the ideal model with $J_p = C_i\, dV_e/dt$, (2) similar, but with softened transitions or (3) with overshoot and $J_p > C_i\, dV_e/dt$, which indicates that space charge increases. (c) In steady state, the $\Delta\, Q_{p,ss}$ versus voltage V_m characteristics can have different shapes: (1) linear with slope $2C_i$ for the ideal model, (2) with softened transition, (3) with S-shape indicating space charge and (4) with hysteresis behavior. The brightness B is roughly proportional with $\Delta\, Q_{p,ss}$.

Space Charge

Measurements on TFELDs have shown that during operation often a positive space charge ρ is present in the bulk of the phosphor layer (8, 12). The electric field in the phosphor layer is then inhomogeneous. For the electric field near the interface of the phosphor layer we have (11):

$$E(0) = E_p - (1 - \frac{x_{sc}}{d_p})\frac{Q_{sc}}{\varepsilon_p}; \quad E(d_p) = E_p + \frac{x_{sc}}{d_p}\frac{Q_{sc}}{\varepsilon_p}$$

with Q_{sc} the integral of the space charge density and x_{sc} the center of mass of the space charge:

$$Q_{sc} = \int_0^{d_p} \rho(x)dx; \quad x_{sc} = \frac{1}{Q_{sc}}\int_0^{d_p} \frac{x}{d_p}\rho(x)dx$$

The difference between $E(d_p)$ and $E(0)$ is proportional to the total amount of space charge in the phosphor layer.

In order to estimate the influence of the space charge on the charge transfer in steady state, we assume again that the tunnel current is an abrupt function of the field at the cathodic interface. For $V_e > 0$ the cathodic interface is at $x = d_p$, and during charge transfer the field there will be clamped to the threshold field for tunneling: $E(d_p) = E_t$. Because of the positive space charge, the field decreases monotonously toward the anode, as can be seen from Eq. (1), and the average field E_p is smaller according to Eq. (10). If we assume that the space charge distribution $\rho(x)$ is not time-dependent, then the transferred charge for a steady state voltage with amplitude V_m is found after combining Eqs. (6) and (10):

$$\Delta Q_{p,ss} = 2C_i(V_m - V_t + \frac{Q_{sc}}{2C_e})$$

Because the creation of space charge is related to charge transfer in the phosphor layer, the space charge is zero below the threshold voltage and increases with the transferred charge $\Delta\, Q_{p,ss}$ until a maximum value is reached (8, 4). The transferred charge versus voltage characteristic has an S-shape, like curve 3 of Fig. (c), and the region with slope larger than $2C_i$ indicates that space charge is present.

OPTICAL BEHAVIOR OF THIN-FILM ELECTROLUMINESCENT DEVICES

The electrons that are transferred through the device will excite dopant atoms in the phosphor layer. The excited dopant atoms can emit a photon with a certain energy, but may alternatively relax to the ground state without radiation. When a photon is generated in the phosphor layer, it can leave the device through the transparent electrode, or be absorbed in the thin-film structure. These three processes are discussed in the following subsections.

Excitation of Dopant Atoms

Dopant atoms in the phosphor layer are normally excited by electrons with sufficient energy which move from the cathodic to the anodic interface in a high electric field. One electron can excite many dopant atoms along its path, because it gains an energy of about 100 eV in the electric field, where only a few electron volts are needed for the excitation process. When $c[m^{-3}]$ is the concentration of dopant atoms and $\sigma[m^2]$ the effective cross section of the dopant atom for excitation, then one electron will on average cause $\sigma\, cd_p$ excitations. To a first approximation this value is proportional with the dopant concentration. However, when the dopant concentration is too large, the electrical properties of the phosphor may change and reduce σ, or nonradiative decay may occur. The cross section for excitation $\sigma[m^2]$ depends on the kind of dopant atom and on the electric field in the phosphor layer. Typical values for Mn are $2 \cdot 10^{-20}$ m^2 for σ and $2.5 \cdot 10^{26}$ m^{-3} for c (7).

In the case of SrS:Ce, some light emission is due to a two-step process: first the Ce atom is ionized by the electron current and later a photon is emitted when the ionized Ce atom captures an electron (15, 16). Electron capture occurs mainly when the electric field is low, and often a trailing edge light peak is observed after the voltage has reached its maximum value. This light peak is due to electrons which are not captured in deep interface states near the anodic interface, and return to the bulk when the field near the anode changes sign. In some cases a trailing edge current peak also has been observed (16).

Radiative Decay

A dopant atom in the excited state can return to the ground state in different ways. It can make a radiative transition and emit a photon with certain energy and wavelength, or it can return nonradiatively. The probabilities for the different transitions depend on the crystal structure and on the presence of impurities or other dopant atoms in the neighborhood (3, 7). For the ZnS:Mn phosphor the emission spectrum has a maximum at 585 nm (yellow/orange), with a full width at half maximum (FWHM) of about 50 nm. The ZnS:Tb spectrum has emission peaks at 490 nm, 545 nm, 590 and 620 nm, each with a FWHM of about 20 nm. The typical emission spectrum of SrS:Ce has a primary peak at 495 nm and a smaller one at 555 nm, each with

a FWHM of about 50 nm. At low dopant concentrations, the decay is nearly exponential, with typical decay times of the order of 10^{-3} s for Mn and Tb, and 10^{-8} s for Ce. For Mn concentrations larger than 1 mol%, nonradiative processes are dominant and the decay becomes faster and nonexponential. More information about luminescence in phosphor materials and about radiative and nonradiative transitions in rare earth ions (like Tb) and in transition metal ions (like Mn), is available in the literature (17).

Outcoupling of Light

The index of refraction of the phosphor material is higher than one (2.3 for ZnS), so only a fraction of the generated light (5% for ZnS) falls inside the emission cone and is emitted into air (1). The rest of the light is either trapped in the substrate by total internal reflection or absorbed by the electrodes. The use of a reflective electrode material like Al enhances the light output through the transparent electrode, but has the disadvantage in that it gives the device a reflective appearance. In many cases the phosphor layer is not optically flat and additional light is emitted due to scattering. Reflection and scattering reduce the contrast between on and off devices under ambient illumination. The contrast can be improved by using a black layer instead of a reflector at the back side, or by covering the front side with a circular polarizer.

Power, Brightness, and Efficiency

During one half period, a charge $\Delta\ Q_{p,ss}$ is transferred through the phosphor layer in an average field $|E_p|$. If the frequency of the periodic voltage is $f[Hz]$, and we use the ideal model described above with $|E_p| = E_t$, then the power $P[W/m^2]$ dissipated by the TFELD is given by (1, 14):

$$P = 4\ f\ \frac{C_i^2}{C_i + C_p}(V_m - V_t)V_t$$

To obtain the brightness $B[cd/m^2]$ the previous expression must be multiplied by the conversion efficiency of the device $\eta[lumen/W]$, and divided by π, if we assume a Lambertian emission:

$$B = \frac{4}{\pi}\ \eta\ f\ \frac{C_i^2}{C_i + C_p}(V_m - V_t)V_t$$

Usually the efficiency does not depend too much on the amplitude of the voltage, so the $B - V_m$ characteristics are similar to the $\Delta\ Q_{p,ss} - V_m$ characteristics of Fig. 4(c). Typical values for monochrome ZnS:Mn devices are $f \cong 60$ Hz, $P \cong 60$ W/m^2, $\eta \cong 5$ lumen/W (corresponding to 1% power efficiency), and $B \cong 100$ cd/m^2. As displays have a limited fill factor and there is also power dissipation in the driver circuits, the total power needed to drive a display with the same average brightness is considerably higher.

THIN-FILM ELECTROLUMINESCENT COLOR DISPLAYS

The first commercial thin-film electroluminescent displays appeared on the market in the mid 1980s. These displays were monochrome orange-yellow displays using ZnS:Mn as the phosphor. These displays are still manufactured today (2006) by the same companies: Sharp Corporation (http://sharp-world.com) and Planar Systems (http://www.planar.com). A typical size is 25 cm in diagonal, with 640 column electrodes and 480 row electrodes. Only Planar introduced also color displays to the market (18, 19).

Different technological approaches are used for the production of the displays (1, 7). Usually the substrate is glass and transparent indium-tin-oxide is used for the electrode on the substrate side. The insulator materials (like AlTiO, SiON, or Al_2O_3) can be deposited by electron-beam evaporation, sputtering, or atomic layer epitaxy. The phosphor materials are deposited by thermal evaporation, electron beam evaporation, or atomic layer epitaxy (2).

For making a full-colour TFEL display one needs efficient red, green and blue emitting phosphors. At the beginnning of the 1980s ZnS doped with different rare-earth elements was investigated and this turned up ZnS:Tb as an efficient green emitter. Then the alkaline earth sulfides CaS and SrS were considered as hosts leading to the discovery of CaS:Eu for "red" and SrS:Ce with a blue/green emission. With an extra blue filter the latter could be used as the "blue" phosphor. Later the cerium-doped thiogallates $CaGa_2S_4$:Ce and $SrGa_2S_4$:Ce and also SrS:Cu,Ag were found which have a more pure blue emission and thus need no filtering, but their efficiency was still too low. At about this time Planar developed the first full-colour TFEL display (22). It consisted of 2 complete TFEL-stacks on two substrates facing each other: a blue display using $CaGa_2S_4$:Ce and a red/green display using ZnS:Mn+filter for "red" and ZnS:Tb for "green". In this way the poor efficiency of the "blue" could be compensated by increasing the area covered by the $CaGa_2S_4$:Ce. In 1999 the L_{40} luminance (40 V above threshold) at 60 Hz was 100 cd/m^2 for ZnS:TbOF (green), 70 cd/m^2 for ZnS:Mn+filter (red) and 28 cd/m^2 for SrS:Cu,Ag (blue) (23). However it became clear that the progress obtained in thin-film phosphor development was too slow to be able to compete with liquid-crystal displays (25). Moreover the structure where each pixel is made up of three different phosphors is probably too complex to become economically viable. A much simpler structure is obtained if a "white" phosphor could be used combined with color filters, similar with a liquid-crystal display, since now no patterning of the phosphors is needed anymore. At that time the best candidate for such a white phosphor was the combination of a ZnS:Mn layer with a SrS:Ce layer (20–18). However this "color-by-white" approach reduces the efficiency at least with a factor 1/3 and therefore needed even better phosphors.

This state-of-affairs probably explains why many research groups active in thin-film electroluminescence gradually stopped their activities. On the other hand two developments took place which will likely prove to be decisive for the future of the TFEL-technology. (i) The Canadian company Westaim developed a hybrid thick-film/thin-film technology (acronym TDEL = thick dielectric EL) in which the first electrode layer and the bottom 20 μm thick insulator layer, which also has a high dielectric constant, are deposited by screen-printing (10, 18). The light generated in the phosphor layer is then emitted through the last de-

posited electrode. (ii) At Meiji University, Japan, a new efficient blue phosphor $BaAl_2S_4$:Eu was developed (24). In the subsequent years the luminance of this phosphor was improved and now (2006) has reached 800 cd/m^2 at a frequency of 60 Hz (26).

Using this new efficient blue phosphor iFire Technology (Westaim's EL division) introduced a new way for making EL color displays: "color-by-blue" (27). In this scheme only a single uniform "blue" phosphor layer is used and the "green" and "red" are obtained by (patterned) color conversion layers where the blue light is down converted by photoluminescence. This structure has the same simplicity as the "color-by-white" approach but does not waste as much energy. Together with its partners Sanyo Electric Co. and Dai Nippon Printing Co., iFire has set-up a pilot-line for the fabrication of 34" TV-panels using this technology.

Besides the sulfur based phosphors, oxide phosphors are now also getting some attention, since they have a higher chemical stability, whereas the sulfides are moisture-sensitive. Oxide phosphors have for a long time been used in fluorescent lamps, plasma display panels and field emission displays, but their application in EL displays is rather new (28). Typically a $BaTiO_3$ sheet is used as substrate on which the phosphor layer is grown by sputtering. The structure is completed with a transparent ZnO:Al electrode on the front side and an Al-electrode on the back side of the substrate. Good results have been obtained with Zn_2SiO_4:Mn, $ZnGa_2O_4$:Mn, Ga_2O_3:Mn, Ga_2O_3:Eu, Y_2O_3:Mn and some mixtures of these materials (28). Usually a high temperature heat-treatment is needed to make the as-deposited amorphous phosphor film crystalline although lowering the processing temperature is looked for (29). Oxide films can also be deposited by simple other than vacuum processes like sol-gel technology combined with dip- or spin-coating (30, 31).

BIBLIOGRAPHY

1. Y. A. Ono, *Electroluminescent Displays*, Singapore: World Scientific, 1995.
2. A. H. Kitai (ed.), *Solid State Luminescence: Theory, Materials, and Devices*, London: Chapman & Hall, 1993.
3. F. Williams (ed.), Workshop on the physics of electroluminescence, *J. Lumin.*, **23**: 1–2, 1981.
4. A. G. Fischer, Electroluminescence in II-VI compounds, inP. Goldberg (ed.), *Luminescence of Inorganic Solids*, New York: Academic, 1966.
5. A. Vecht and N. J. Werring, Direct current electroluminescence in ZnS, *J. Phys. D: Appl. Phys.*, **3**: 105–120, 1970.
6. T. Inoguchi and S. Mito, Phosphor films, inJ. I. Pankove (ed.), *Electroluminescence*, Berlin: Springer-Verlag, 1977.
7. R. Mach and G. O. Mueller, Physical concepts of high-field thin-film electroluminescent devices, *Phys. Stat. Sol. (a)*, **69**(11): 11–66, 1982.
8. W. E. Howard, O. Sahni, and P. M. Alt, A simple model for the hysteretic behavior of ZnS: Mn thin film electroluminescent devices, *J. Appl. Phys.*, **53**: 639–647, 1982.
9. E. Bringuier, Tentative anatomy of ZnS-type electroluminescence, *J. Appl. Phys.*, **75**: 4291–4312, 1994.
10. X. Xurong (ed.), Proceedings of the 7th International Workshop on Electroluminescence in Beijing, Beijing: Science Press, 1996.
11. K. Neyts *et al.*, Observation and simulation of space charge effects and hysteresis in ZnS: Mn ac thin-film electroluminescent devices, *J. Appl. Phys.*, **75**: 5339–5346, 1994.
12. K. Neyts,Interpretation of time resolved measurements on ac thin film electroluminescent devices,
13. *Technical Digest of the Int. Symp. on Inorganic and Organic Electroluminescence in Hamamatsu*, 1994, pp. 30–35.
14. P. M. Alt, Thin film electroluminescent displays: device characteristics and performance, *Proc. S.I.D.*, **25**(2): 123, 1984.
15. H. Yoshiyama *et al.*, Excitation mechanism based on field-induced delocalization of luminescent centers in CaS:Eu^{2+} and SrS:Ce^{3+} thin-film electroluminescent devices, inS. Shionoya andH. Kobayashi (eds.), *Electroluminescence: Proceedings of the Fourth International Workshop, Tottori, Japan*, New York: Springer-Verlag, 1989, pp. 48–55.
16. K. Neyts and E. Soininen, Space charge and light generation in SrS:Ce thin film electroluminescent devices, *IEEE Trans. Electron Devices*, **42**: 1086–1092, 1995.
17. G. Blasse and B. C. Grabmaier, *Luminescent Materials*, Berlin: Springer-Verlag, 1994.
18. R. H. Mauch andH.-E. Gumlich (eds.), *Inorganic and Organic Electroluminescence/EL 96 Berlin*, Berlin: Wissenschaft und Technik Verl., 1996.
19. W. Barrow *et al.*, A high contrast, full color, 320.256 line TFEL display, in Conf. Record of the 1994 Int. Display Research Conf. (SID), 1994, pp. 448–451.
20. K.- O. Velthaus *et al.*, High luminance ZnS:Mn/SrS:Ce TFEL devices, in Conf. Record of the 1994 Int. Display Research Conf. (SID), 1994, pp. 346–349.
21. A. Mikami *et al.*, Aging characteristics of ZnS:Mn electroluminescent films grown by a chemical vapor deposition technique, *J. Appl. Phys.*, **72**: 773–782, 1992.
22. R. T. Tuenge, Recent Progress in Color Thin Film EL Displays, Asia Display '95, Proc. of the 15th Int. Display Res. Conf.,pp. 279–282, 1995.
23. R. Tuenge,Inorganic electroluminescent displays, SID Seminar Lecture Notes, F-4/1–33, 1998.
24. N. Miura *et al.*, High-Luminance Blue-Emitting $BaAl_2S_4$:Eu Thin-Film Electroluminescent Devices, *Jpn. J. Appl. Phys.*, **38**: L1291–L1292, 1999.
25. C. King, History of TFEL Technology at Planar Systems, Proc. 11th Int. Workshop on Inorganic and Organic Electroluminescnece & 2002 Int. Conf. on the Science and Technology of Emissive Displays and Lighting, 2002, Gent, Belgium, pp. 5–10.
26. N. Miura, Phosphor Studies for Color EL Devices, Proc. 13th Int. Workshop on Inorganic and Organic Electroluminescnece & 2006 Int. Conf. on the Science and Technology of Emissive Displays and Lighting, 2006, Jeju, Korea, pp. 240–242.
27. X. Wu *et al.*, Color-by-Blue: A novel method to achieve full-color inorganic EL displays, *J. of the SID*, **12**(3),p. 281, 2004.
28. T. Minami, Oxide thin-film electroluminescent devices and materials, *Solid-State Electronics*, **47**(2003),pp. 2237–2243.
29. A. H. Kitai, Oxide phosphor and dielectric thin films for electroluminescent devices, *Thin Solid Films*, **445**(2003),pp. 367–376.

30. T. Minami *et al.*, Electroluminescent Devices with Ga_2O_3:Mn Thin-Film Emitting Layer Prepared by Sol-Gel Process, *Jpn. J. Appl. Phys.*, **39**(2000),pp. L524–L526.
31. K. Vanbesien *et al.*,Zn_2SiO_4:Mn thin films made with sol-gel technology for electroluminescent displays,
32. Proc. 13th Int. Workshop on Inorganic and Organic Electroluminescnece & 2006 Int. Conf. on the Science and Technology of Emissive Displays and Lighting, 2006, Jeju, Korea, pp. 103–105.

PATRICK De VISSCHERE
KRISTIAAN NEYTS
Ghent University,
Sint-Pietersnieuwstraat 41,
Gent, Belgium